Geomorphology 389 (2021) 107805

Contents lists available at ScienceDirect

Geomorphology

journal homepage: www.elsevier.com/locate/geomorph

Wildfire and the patterns of floodplain large wood on the Merced River, Yosemite National Park, California, USA

Emily P. Iskin *, Ellen Wohl

Department of Geosciences, Colorado State University, Fort Collins, CO 80523-1482, USA

ARTICLE INFO

Article history:
Received 9 September 2020
Received in revised form 13 May 2021
Accepted 24 May 2021
Available online 2 June 2021

Keywords:
Floodplain
Large wood
Wildfire
Spatial distribution

ABSTRACT

We quantified floodplain large wood load (m^3 wood/ha) and spatial distribution on the Upper Merced River in Yosemite National Park, California, USA. The upstream portion of the study area includes a recently burned section of the Merced River corridor and the downstream portion contains floodplain with undisturbed forest, facilitating investigation of the effects of wildfire on floodplain large wood. We used measurements of wood load and spatial distribution to test hypotheses regarding floodplain wood dynamics in the channel versus the floodplain and in burned versus unburned portions of the study area. The median wood load on the Merced River floodplain, as measured along numerous transects, is 259 m^3/ha overall, with non-significant differences between burned (median 196 m^3/ha) and unburned (median 277 m^3/ha) portions of the floodplain. We found that jams can occur across the entire width of the floodplain. Burned wood pieces are present throughout the study area in the channel but are largely absent from unburned portions of the floodplain, despite the occurrence of overbank flows since the wildfire. A greater proportion of large wood is within logjams in burned portions of the floodplain. We infer that wood recruited to the channel via bank erosion moves readily downstream within the channel, whereas wood moving from the channel onto the floodplain concentrates near the margin of the main channel or within secondary channels and depressions on the floodplain, leading to the formation of long, narrow logjams.

© 2021 Elsevier B.V. All rights reserved.

1. Introduction

An extensive literature documents the physical and ecological effects of large wood in active river channels (e.g., Gurnell, 2013; Ruiz-Villanueva et al., 2016b; Wohl, 2017). Large wood (LW) here refers to downed, dead wood pieces ≥10 cm in diameter and 1 m in length (Wohl et al., 2010). Physical effects of LW in channels include altered hydraulics (Gippel, 1995; Bocchiola, 2011), increased flow resistance (Shields and Smith, 1992; Comiti et al., 2008; Wilcox et al., 2011), retention of mineral and organic particulate material (Mao et al., 2008; Beckman and Wohl, 2014), increased hyporheic exchange (Lautz et al., 2006; Fanelli and Lautz, 2008; Sawyer et al., 2012), increased morphological spatial heterogeneity within the channel (Keller and Swanson, 1979; Livers and Wohl, 2016; Wohl, 2016), altered bedforms (MacFarlane and Wohl, 2003), and increased hydrologic connectivity between the channel and floodplain (Jeffries et al., 2003; Brummer et al., 2006; Sear et al., 2010). Ecological effects of instream LW include greater abundance and diversity of habitats and stream biota (Richmond and Fausch, 1995; Herdrich et al., 2018; Nakano et al., 2018), including plants on bars and islands (e.g., Fetherston et al., 1995; Gurnell et al., 2019), and increased nutrient uptake (Battin et al., 2008; Fanelli and Lautz, 2008; Entrekin et al., 2020).

Geomorphic investigation of LW on floodplains lags studies of instream LW, although several recent studies have focused on aspects of floodplain LW. These studies indicate that LW on or within the floodplain can create analogous effects to LW in channels (Wohl, 2013, 2020), including reduced velocity and increased ponding of overbank flow and enhanced sediment deposition on floodplains (Jeffries et al., 2003); enhanced interactions between the channel and floodplain, leading to greater floodplain heterogeneity (Jeffries et al., 2003; Sear et al., 2010; Wohl, 2011b; Collins et al., 2012); increased habitat for terrestrial and aquatic plants and animals (Benke, 2001; Braccia and Batzer, 2001; Dolloff and Warren, 2003; Zalewski et al., 2003; Pettit and Naiman, 2006); and increased organic carbon stock (Lininger et al., 2017; Scott and Wohl, 2018).

Large wood regimes characterize wood recruitment, transport, and storage in river corridors (Wohl et al., 2019); river corridor here refers to the active channel and floodplain. Wood recruitment on floodplains can come from adjacent uplands, from the floodplain forest (e.g., Lassettre et al., 2008), and from fluvial transport onto the floodplain (Wohl, 2020). Floodplain wood can be transported out of the floodplain or redistributed on the floodplain by overbank flows (Piégay, 1993; Wohl, 2013). Redistribution on the floodplain tends to

---

* Corresponding author.
E-mail address: Emily.Iskin@colostate.edu (E.P. Iskin).

https://doi.org/10.1016/j.geomorph.2021.107805
0169-555X/© 2021 Elsevier B.V. All rights reserved.

occur at the entrance and exit of secondary channels (Piégay, 1993; Piégay and Marston, 1998; Wohl et al., 2018b), along the channel margins in densely forested floodplains (Piégay and Gurnell, 1997; Piégay, 2003), and around standing trees across the floodplain on sparsely forested floodplains (Wohl et al., 2018a).

Wildfire can also influence the wood regime on floodplains, although the effects are highly dependent on the combined influences of the floodplain vegetation seral stage, the temporal sequence of fires, the time since the most recent stand-killing fire, and the intensity of the fire (Dwire and Kauffman, 2003). Seral stage influences the size distribution of trees killed by the fire and available for recruitment as LW, as well as the susceptibility of burned trees to falling (e.g., Bendix and Cowell, 2010). Temporal sequence of fires also influences the abundance of dead wood. Donato et al. (2016), for example, found that in conifer forests of Oregon, USA two fires within 15 years of each other resulted in 45% less dead wood mass (standing plus down) than a single fire. Time since the most recent stand-killing fire influences rate of topple of snags (standing dead trees), although details vary with fire intensity and type of forest. Fire intensity governs mortality of living trees and whether downed wood is partially or completely burned. In general, multiple studies indicate that wood recruitment through toppling of fire-killed trees increases wood loads (e.g., Chen et al., 2005; Marcus et al., 2011; Short et al., 2015; Lininger et al., 2017; Picco et al., 2021) although individual wood piece size may decrease (e.g., Berg et al., 2002). The time to maximum increase in wood load after fire varies among studies. Wood recruitment to the river corridor can also increase following wildfire because of hillslope mass movements that include wood, increased bank erosion, and altered rainfall-runoff-sediment yield relations and channel aggradation that increase the magnitude and frequency of overbank flows, as well as toppling of fire-killed trees (e.g., Young, 1994; Benda et al., 2003; Wohl et al., 2020).

Wildfire is a substantial disturbance in the California Sierra Nevada (Skinner and Chang, 1996; Berg et al., 2002). Previous studies of wildfire effects in the region, however, have not examined how wildfire influences the movement of large wood between the channel and floodplain and the resulting differences in floodplain wood load and spatial distribution of wood. We used a study area in the Upper Merced River of California's Sierra Nevada to quantify the wood load and spatial distribution of floodplain large wood (LW) and to investigate whether LW characteristics differ between upstream portions of the study area that burned in 2014 and downstream unburned portions of the study area. We hypothesized that:

H1. There is a greater LW load on the floodplain in unburned areas than in burned areas. This reflects the assumption that wildfire kills living trees and consumes existing LW. This hypothesis is worth testing because previous studies indicate mixed results and suggest that fire could increase the floodplain LW load by increasing tree mortality but not causing complete combustion of downed wood.

H2. There are more floodplain logjams close to the active channel in both burned and unburned portions of the floodplain. A concentration of floodplain jams close to the channel margins could reflect one or more scenarios. First, bank erosion creates channel-marginal jams that subsequently accrete to the floodplain. Second, transport capacity declines with distance from the channel during overbank flow because of the combined effects of (i) lateral transfer of momentum from deeper, faster flow in the channel to shallower, slower flow on the floodplain (Knight and Shiono, 1996), (ii) shallower flows farther from the channel if distal parts of the floodplain are at slightly higher elevation, and (iii) greater surface roughness and obstructions associated with floodplain vegetation, including standing live and dead trees (e.g., Ruiz-Villanueva et al., 2016a). This hypothesis is worth testing because previous studies indicate highly competent wood transport across the entire floodplain in sparsely forested sites (Wohl et al., 2018a) versus limited and localized wood transport across the floodplain in more densely forested sites (Piégay and Gurnell, 1997; Wohl et al., 2018b). However, the threshold separating extensive and localized wood transport and deposition across forested floodplains has not yet been defined and additional field data are needed to constrain this threshold.

H3. There are burned pieces of LW throughout the length of the active channel in the study area. This hypothesis reflects the inference that the active channel has a high transport capacity for LW, allowing wood to be distributed from the upstream burned area to downstream unburned areas. In addition, previous studies indicate that burned wood pieces can be highly mobile because of the combined effects of smaller piece size, greater runoff from burned areas, and channel instability following wildfire (e.g., Young, 1994; Zelt and Wohl, 2004).

H4. Burned LW on the floodplain is present only within burned portions of the floodplain. This contrasts with hypothesized patterns of burned LW distribution in the active channel (H3) and reflects the inference that the floodplain has a lower transport capacity for LW than the channel, which limits downstream transport of burned wood on the floodplain and transfer of burned wood from the channel to the floodplain. Ability to test this hypothesis depends on the occurrence of overbank flows since the wildfire. Such flows have occurred, as described under Study area.

H5. There is a greater proportion of floodplain LW in jams in burned areas than in unburned areas. This reflects the inference that, if wildfire consumes floodplain LW and ground cover, the associated reduced floodplain roughness facilitates LW transport onto the floodplain and the formation of jams.

Testing these hypotheses provides insight into LW dynamics in burned and unburned portions of a floodplain. Specifically, we can evaluate the net effect of wildfire on floodplain wood load and spatial distribution relative to unburned portions of the study area five years after the fire, and we can examine the relative importance of floodplain tree mortality versus fluvial transport of LW onto the floodplain. Time since the fire and since the last high flow that significantly inundated the floodplain influence what we observed and measured. The study area is not a perfect natural laboratory because the floodplain is wider in the burned area than in the unburned area. Although both burned and unburned portions of the floodplain include depressions and secondary channels that are inundated during annual snowmelt peak flows, and both portions have been subject to the same flow magnitudes since the fire, we do not have high-resolution topographic data for the whole study area and cannot demonstrate that hydrologic connectivity is consistent along the length of the study area. However, we can gain useful insights by comparing patterns of wood load and deposition between the burned and unburned portions of the floodplain. The final part of the paper compares the floodplain wood loads in the study area to published values for other field sites and presents a conceptual model of variations in floodplain wood load with time since a stand-killing wildfire.

2. Study area

The study area extends along ~5 km of the Merced River upstream of Nevada Falls in Yosemite National Park, California, USA (Fig. 1). The Merced River here drains 300 km^2 and is a medium-large river with respect to LW dynamics (Gurnell et al., 2002), in that only a few pieces of LW are sufficiently long to span the active channel. The study area is underlain primarily by Holocene alluvium, with Holocene talus including moraines and rock glaciers and Half Dome Granodiorite in the Late Cretaceous Tuolumne Intrusive Suite underlying parts of the area (Peck, 1964, 2002).

The study area is within the upper montane zone. Deciduous trees and shrubs, including such species as black cottonwood (*Populus trichocarpa*), quaking aspen (*Populus tremuloides*), and western azalea

Fig. 1. Study area and inset map showing the location within the contiguous United States. Latitude (N) and longitude (W) coordinates indicated at lower left margin. Blue arrow indicates flow direction. The burned portion of the floodplain appears as pale brown in the lower image.

(*Rhododendron occidentale*), grow next to the river, on the floodplain, and in wetland areas (Hall, 1921). Conifer species including Jeffrey pine (*Pinus jeffreyi*), incense cedar (*Libocedrus decurrens*), and Douglas-fir (*Pseudotsuga menziesii*) are present in all parts of the river corridor (Hall, 1921). The conifers, which supply LW to the river corridor, attain a maximum height of 50–60 m. The systematic record of wildfires in Yosemite National Park dates to 1930 (National Park Service, 2019). The only large and/or long-duration fire in the study area since 1980 was the Meadow Fire in 2014. The portion of the floodplain burned in this fire now generally has less dense foliage than the unburned areas of the floodplain and valley bottom (Supplemental Figs. 1 and 2). The valley walls in the study area are largely bedrock (Supplemental Fig. 1), which limited mass movements following the fire. We did not see evidence of substantial LW introduction to the floodplain via hillslope instability; floodplain LW recruitment appears to result primarily from tree topple and fluvial transport onto the floodplain.

Mean annual precipitation is 120 cm. California has a Mediterranean climate with hot, dry summers and cool, wet winters. In the Sierra Nevada, afternoon thundershowers can bring summer precipitation to the mountains, but the Merced River flow regime is dominated by a single annual flood caused by snowmelt runoff that peaks during May or June. The US Geological Survey StreamStats program estimates the two-year peak flood at the study area as 42.5 m^3/s. The nearest stream gage is downstream of the study area by ~4 km (USGS stream gage 11264500, drainage area 470 km^2), and although there are tributaries between the downstream end of the study area and the gage and it does not provide precise data, this gage does provide information on the timing and relative magnitude of peak flows. Using USGS data from 1915 to 2019 at this gage (U.S. Geological Survey, 2020), we calculated the mean water year (October 1–September 30) discharge recurrence interval during the 2019 field work to be 8 years. This was completed by ordering the annual data from most discharge to least and assigning ranks starting with 1, and calculating the recurrence interval as $RI = \frac{Total\ number\ of\ years\ with\ data+1}{Rank\ of\ that\ year}$. During the period 2014–2019 (i.e., between the wildfire and field work), the years 2017, 2018, and 2019 had peak flows exceeding the long-term median peak flow value of 76 m^3/s (Supplemental Fig. 3).

The 5-km-long study reach was chosen specifically because of the (1) limited access, except by foot, which has helped to preserve the relatively natural conditions during the period of resource exploitation prior to establishment of the national park and subsequent development of infrastructure for motorized travel in the park, (2) the existence of natural boundaries (waterfalls) at both ends of the reach and relatively consistent valley-bottom geometry within the reach, and (3) the presence of distinctly different floodplain forest stand characteristics as a result of the 2014 Meadow Fire. We focus on the right side of the floodplain because an established foot trail made this portion of the study area readily accessible, whereas steep terrain on the left bank and a river too deep to cross on foot rendered the left bank largely inaccessible.

The Merced River within the study area has an average reach-scale gradient of 0.021 m/m. Median bankfull channel width is 31 m, with individual subreach medians ranging from 23 to 37 m (Supplemental Table 1). The 5 km of river corridor was partitioned into 8 subreaches (Fig. 2) based on Google Earth aerial photos and field-delineated discontinuities in geomorphic parameters including channel gradient, sinuosity, floodplain width, and floodplain vegetation. Subreaches 1 through 5 (numbered sequentially starting at the upstream end) burned in the 2014 Meadow Fire. Median floodplain width varies significantly between the burned area (107 m; range 3–267 m) and the unburned area (8 m; range 0–44 m).

3. Methods

We conducted field work on the Merced River during summer 2019. We used measurements on the ground and from aerial photos (from 2014 in Google Earth) to derive several variables used in statistical analyses to test the hypotheses. These variables describe the geomorphology and forest characteristics of the river corridor and the characteristics of LW (Table 1). Locations of river corridor and subreach boundaries, transects, and logjams were measured using a Garmin eTrex 10, with varying horizontal accuracy (maximum ±3 m).

We measured the diameter of every piece of LW and the dimensions of all logjams intersected by floodplain transects that extended from the

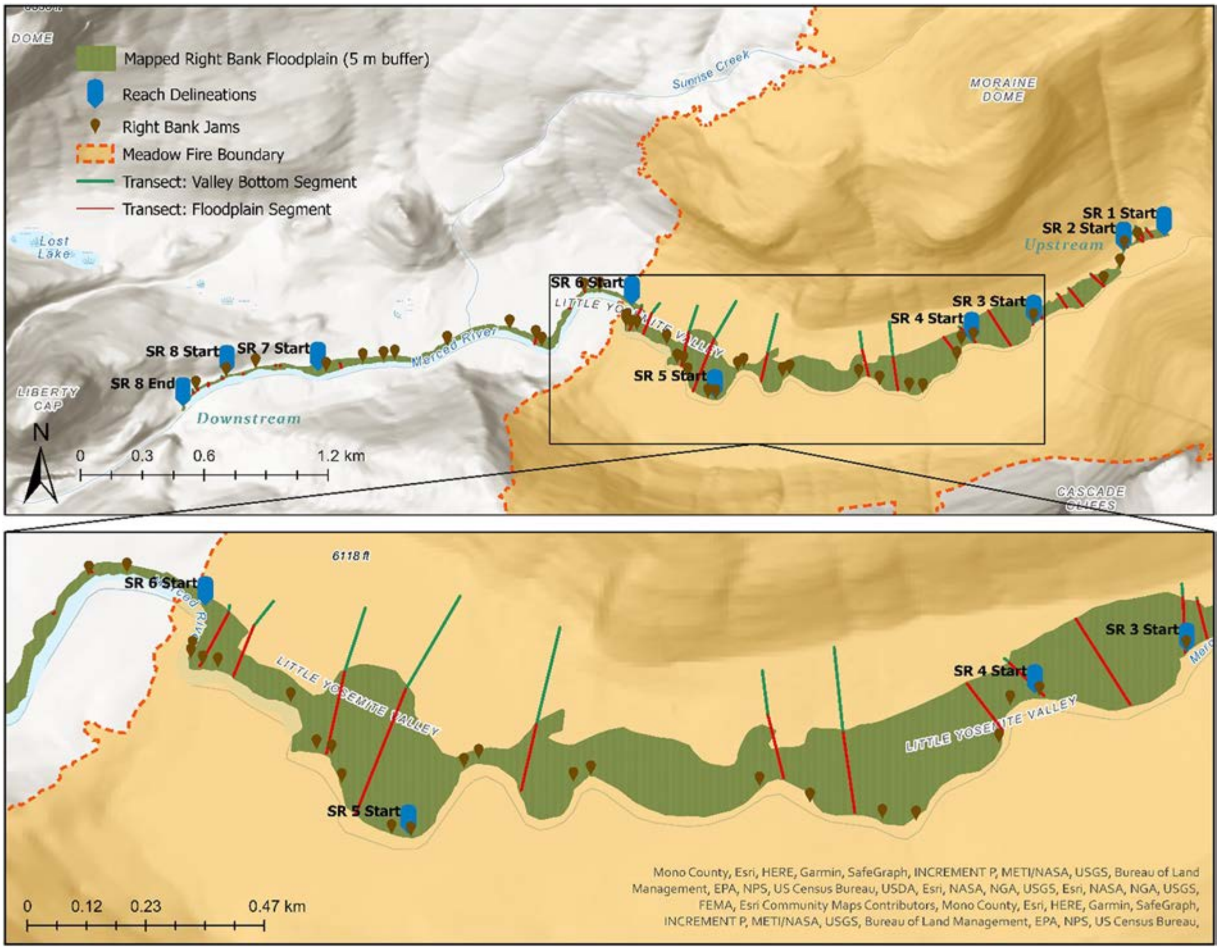

Mono County, Esri, HERE, Garmin, SafeGraph, INCREMENT P, METI/NASA, USGS, Bureau of Land Management, EPA, NPS, US Census Bureau, USDA, Esri, NASA, NGA, USGS, Esri, NASA, NGA, USGS, FEMA, Esri Community Maps Contributors, Mono County, Esri, HERE, Garmin, SafeGraph, INCREMENT P, METI/NASA, USGS, Bureau of Land Management, EPA, NPS, US Census Bureau,

Fig. 2. Study area map including the right bank floodplain, subreach boundaries (SR 1, etc.), instream logjam locations, 2014 Meadow Fire boundary, and location of floodplain/valley bottom transects.

right bankfull channel edge to the back boundary of the valley bottom, following methods in Wohl et al. (2018b). We define the active channel as bounded by the bankfull indicators of presence of terrestrial vegetation, high water marks (e.g., fine organic debris), and change in bank angle. We defined the floodplain as the fluvially created, low-relief surface on either side of the active channel which is inundated by floods that recur at least every few years. The floodplain has erosional and depositional features indicating recent overbank flow and riparian and wetland vegetation communities. At each floodplain transect, we delineated the inner edge of the valley bottom as the boundary of the 2019 inundated floodplain based on high water marks and fluvial erosional and depositional features. The outer edge or back boundary of the valley bottom was the point at which the elevation started to increase significantly from that of the floodplain (e.g., at a bedrock or sediment-mantled hillslope or an alluvial terrace).

All statistics were run in either RStudio (R Core Team, 2019) or Microsoft Excel (simple averages, maxima, minima). NAs were removed for all summary statistics and tests were run in R (Table 2). Although the transects were nested within the subreaches, this was not considered for the statistical analyses. An $\alpha = 0.05$ was used for all tests of significance.

4. Results

The dataset included 1345 pieces of LW across the active channel, floodplain, and valley bottom and 28 logjams measured along floodplain transects (burn class was only noted for pieces of LW in logjams, and therefore the following analyses regarding burn class do not include individual pieces of LW not in jams). Supplemental Table 1 summarizes salient features of the study area. Among the notable features is a relatively abrupt decrease in floodplain width that corresponds to the boundary between the burned and unburned portions of the study area (between subreaches 5 and 6). There is no obvious geologic structure that explains this decrease in floodplain width, but the presence of this change complicates our ability to understand the effects of wildfire on floodplain wood dynamics in the study area because the widths of the floodplain (Wilcoxon test p-value <0.001) and valley bottom (Wilcoxon test p-value <0.001) are statistically different between burned and unburned areas. Median floodplain width is 107 m in the burned area and 8 m in the unburned area. (The bankfull channel width (Wilcoxon test p-value >0.05) and channel gradient, however, do not differ significantly between burned and unburned areas.)

Despite the impression that the density of standing trees is lower in the burned area (Supplemental Figs. 1 and 2), the basal area did not differ significantly between burned and unburned portions of the floodplain (p-value $= 0.15$). The distribution of LW diameters differs among channel, floodplain, and valley bottom locations, both in median diameter comparisons and in the distributions of LW diameters. The median diameter of LW in the channel ($n = 388$) is significantly larger than that of both the floodplain ($n = 779$) and valley bottom ($n = 178$) based on statistical comparisons using Kruskal-Wallace (p-value <0.001) and post hoc Dunn's tests (p-value $_{(\mathrm{BF\text{-}FP})} = 0$, p-value $_{(\mathrm{BF\text{-}VB})} = 0$, p-value $_{(\mathrm{FP\text{-}VB})} = 0.33$). The piece size distributions of LW diameters in each location are also slightly different ($\mathrm{sd}_{\mathrm{BF}} = 0.13$, $\mathrm{sd}_{\mathrm{FP}} = 0.10$, $\mathrm{sd}_{\mathrm{VB}} = 0.12$) with variances that differ significantly (Brown-Forsythe, p-value <0.001, $\mathrm{var}_{\mathrm{BF}} = 0.018$, $\mathrm{var}_{\mathrm{FP}} = 0.010$, $\mathrm{var}_{\mathrm{VB}} = 0.014$).

Table 1
River corridor and large wood variables used in statistical analyses.

Category	Variable (units)	Description & sample size	Method
River corridor	Sinuosity, S (m/m)		Calculated using Google Earth imagery
	Bankfull width, BFW (m)	Measured perpendicular to the general trend of the river at every 50 m downstream	Laser rangefinder, metric tapes, Google Earth imagery
	Floodplain width, FPW (m)		
	Valley bottom width, VBW (m)		
	Subreach, SR	n = 8	Designated on Google Earth based on visible longitudinal changes, especially changes in floodplain forest cover, short reaches with islands or bars, and notably large logjams. Designations were confirmed or re-established using ground-based observations.
	Transect, T	4 in each subreach, n = 32	
	Basal area standing trees, BA	Measured on floodplain & valley bottom, n = 32	Counted using Panama angle gage, standard forestry tool for measuring forest stand density
Large wood	Diameter, D (m)	Diameter at breast height	Metric hand tape and visual estimation
	Length, L (m)		Metric tape and visual estimation
	Distance from bankfull edge of active channel, DR (m)		Laser Technology TruPulse 360° laser rangefinder (accuracy of 0.03 m)
	Burn class, BC 0-2	0 no visible burn; 1 some visible burn; 2 burned to the core	
	Decay class, DC 1–5	1 needles/leaves, branches, bark present; 2 finer branches, no needles present; 3 no branches or bark, firm; 4 some decay, not soft; 5 soft, can pull apart with hands	Visual/physical estimate, adapted from Wohl et al. (2010)
	In jam	Jam? Y/N	
	Jam Size:		
	Jam length, JL (m)	Parallel to channel, n = 281	Laser rangefinder, hand tapes
	Jam width, JW (m)	Perpendicular to channel	
	Jam height, JH (m)	Perpendicular to ground	
	Jam porosity, p (%)		Visual estimation (Livers and Wohl, 2016)
	Wood load, WL (m^3/ha)	Calculated for each transect across the floodplain & valley bottom, & for each subreach of the bankfull channel	Line intersect method (Van Wagner, 1968) & piece-based calculations

Fig. 3 illustrates the distribution of LW by subreach and transect by showing distance from the bankfull edge for every piece of LW on the floodplain. The single dots are dispersed pieces and the dots that form a horizontal line indicate the location of a floodplain logjam (all pieces of LW in the jam were marked as being in the same location). This distribution shows that subreaches 3 through 5 had LW farther away from the channel and had the widest floodplains. Many of the floodplain jams line up horizontally between adjacent subreaches, indicating that there are areas of the floodplain with more competent flow and/or shallow, secondary channels on the floodplain. This aligns with field observations of subtle complexities in topography and development of secondary channels on the floodplain, especially on the wider floodplains of the burned area (Supplemental Fig. 2).

Table 2
Summary of statistical tests.

Statistical test	Description	Hypothesis tested
Wilcoxon rank sum test (without ties)[a]	Non-parametric approximate test of equality of two medians; useful for non-normal data[b]	H1
Exact Wilcoxon-Mann-Whitney test (with ties)[a,c]		H1
Brown-Forsythe test[d]	Test for equality of variances using the median as the measure of center; useful for non-normal data[b]	H1
D'Agostino test of skewness[e]	Test for skewness, null hypothesis is that the data are normally distributed with skew = 0	H2
Pearson's chi square test for contingency tables	Test of association between variables, also gives expected values[b]	H3, H5
Odd ratio with Wald method[f]	Describes the strength of association between variables[b]	H3, H5
Fisher's Exact test	Test of association between variables for contingency tables with small values[b], also gives odds ratio and confidence intervals	H4

[a] Mostly referred to as Wilcoxon test in text.
[b] Adapted from Hess (2019).
[c] From the coin package (Hothorn et al., 2006).
[d] From the car package (Fox and Weisberg, 2019).
[e] From the moments package (Komsta and Novomestky, 2015).
[f] From the epitools package (Aragon, 2017).

4.1. Hypothesis tests

We hypothesized that there is a greater wood load on the floodplain in unburned than in burned areas (H1). Median values for floodplain wood load were calculated from the total wood loads for each floodplain transect. We compared the wood load (Fig. 4a) and LW diameters (Fig. 4b) on the burned and unburned areas using the data from the 32 floodplain transects.

Wilcoxon test results show that there is no significant difference between the median total transect LW loads in burned vs unburned areas (p-value >0.05), and the variance in LW loads was not statistically different (Brown-Forsythe test, p-value >0.05). Consequently, the results do not support H1. We also found that the median diameter of floodplain LW does not differ between burned and unburned areas (Wilcoxon test, p-value >0.05) and that the variances are homogeneous for the two populations (Brown-Forsythe test, p-value >0.05).

We hypothesized that there are more floodplain logjams close to the active channel in both burned and unburned portions of the floodplain (H2). To test this hypothesis, we plotted the floodplain logjam data against distance from the bankfull edge of the channel expressed as percentage of total floodplain width f (Fig. 5). The boxplot shows a non-skewed distribution and the two-sided D'Agostino test confirms this (skew = 0.102, p-value >0.05). This means that there are not more floodplain jams positioned to either side of the mean than in a normal distribution ($\text{skew}_{\text{normal}} = 0$), indicating no tendency for floodplain jams to be closer to the river when the individual width of each floodplain transect is taken into account. In summary, the results do not support H2.

We hypothesized that there are burned pieces of LW throughout the length of the active channel in the study area (H3). To test this, we compiled the number of LW pieces in logjams within the active channel by burn status of the subreaches (Fig. 6), and by subreach and burn class of the LW itself (Supplemental Fig. 4). The burn class column plot (Fig. 6) shows that all three burn classes of LW (Table 1) are present in portions of the river flowing through burned and unburned areas,

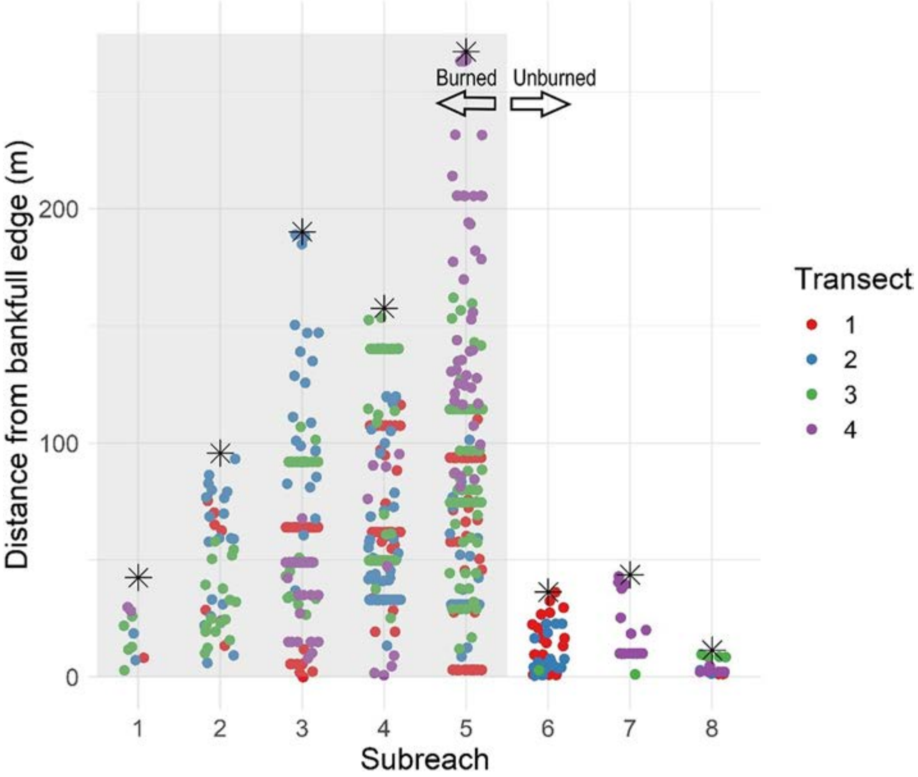

Fig. 3. Location of large wood on the floodplain. The black stars indicate the maximum floodplain width of the four transects for each subreach. Subreaches 1–5 are in the 2014 Meadow Fire burn zone.

although there is more burned LW (burn classes 1 and 2) by count in the burned area. This indicates that burned wood from the burned portions of floodplain is being transported downstream to the unburned subreaches of the channel. Chi square p-value <0.05 indicate that there is an association, and the odds ratio confidence intervals that do not include 1 show that the odds ratio, λ, is statistically significant. In other words, the odds that a burned piece of river LW being in the burned area is 15.6 times as likely as the odds of a burned piece of river LW being in the unburned area (Table 3). The point plot (Supplemental Fig. 4) indicates LW of burn class >0 occurs within each subreach of the river. Thus, the results support H3 and the inference that LW in the river is transported both laterally from the floodplain to the river and longitudinally downstream. The presence of burned pieces of wood in the Merced River downstream of the study area suggests that longitudinal connectivity of wood transport extends farther downstream.

We also hypothesized that burned LW is present only within burned portions of the floodplain (H4). To test this hypothesis, we compiled the number of LW pieces in floodplain logjams by burn status of the subreaches (Fig. 7) and by subreach and burn class of the LW itself.

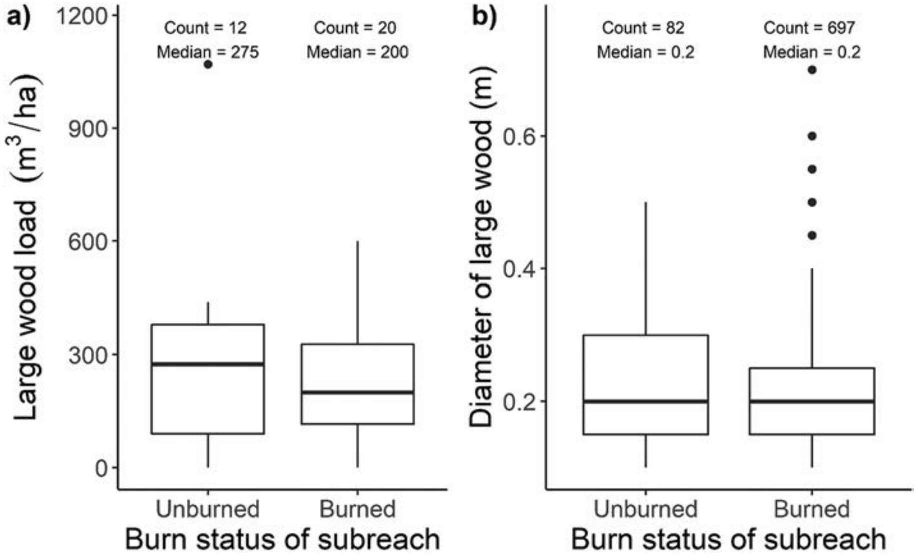

Fig. 4. Comparison of (a) transect large wood load and (b) individual piece diameters on the floodplain by burn status (H1).

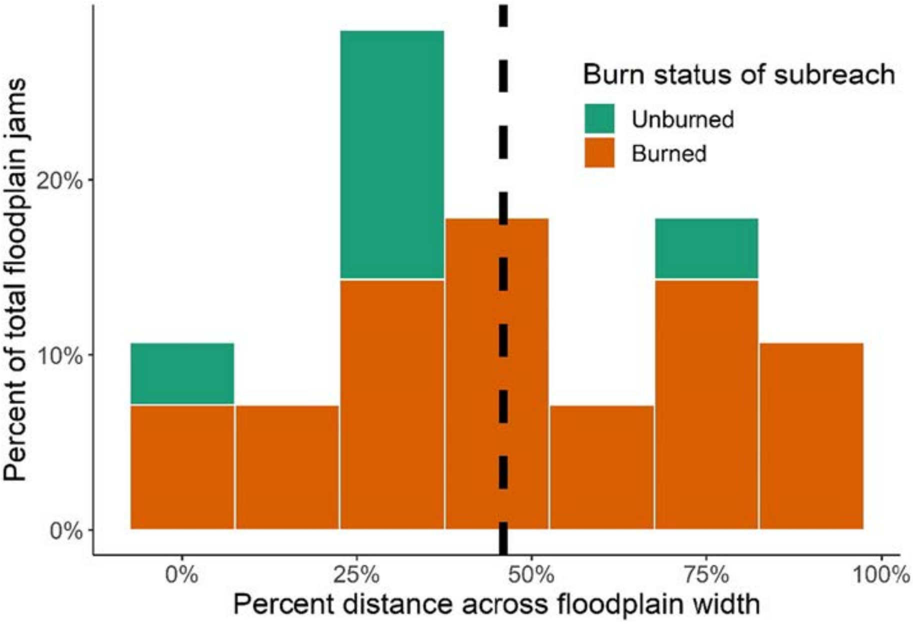

Fig. 5. Distance from the bankfull edge of floodplain jams (H2). Median distance from the river showed by the dashed black line (46.7 m).

The column plot (Fig. 7) indicates that there is only one piece of burned LW in a logjam within the unburned portion of the floodplain. Fisher's Exact *p*-value <0.05 indicates that there is an association, and the odds ratio confidence intervals that do not include 1 show that the odds ratio is statistically significant. Specifically, the odds that a burned piece of floodplain LW being in the burned area is 518 times as likely as the odds of a burned piece of floodplain LW being in the unburned area (Table 3). These results support H4 and the inference that the great majority of movement of LW on the floodplain since the fire has been lateral with respect to the trend of the active channel rather than longitudinally down the floodplain. Lateral movement of LW also appears to reflect relatively limited movement from the channel to the floodplain and limited movement across the floodplain into the unburned zone.

Finally, we hypothesized that there is a greater proportion of floodplain LW in jams in burned areas than in unburned areas (H5). Because the variation in floodplain width between burned (median width 107 m) and unburned (median width 8 m) portions of the study area could bias results of statistical tests, we conducted three distinct

Fig. 6. Burn class of large wood in logjams in active channel by subreach burn status (H3).

Table 3
Results of the hypothesis testing for H3 & H4.

Comparison	Test	*p*-Value	Odds ratio, λ	95% confidence interval	Significant?
Bankfull Channel	χ^2	$<3 \times 10^{-16}$	15.6	8.1, 30.1	Yes
Floodplain	Fisher's Exact	$<3 \times 10^{-16}$	502.3	79.2, 16384	Yes

Table 4
Results of the hypothesis testing for H5.

Comparison	χ^2 *p*-value	Odds ratio, λ	95% confidence interval	Significant?
Full floodplain width	0.0013	2.11	1.33, 3.34	Yes
First 50 m of floodplain	0.00013	2.63	1.59, 4.34	Yes
First 50% of floodplain	0.42	1.26	0.72, 2.20	No

statistical tests for H5: (1) Comparison of the proportions of floodplain LW that were/were not in jams and in burned/unburned areas for the entire floodplain; (2) comparison of the proportions of floodplain LW that were/were not in jams and in burned/unburned areas for only the proximal 50 m of the floodplain; and (3) comparison of the proportions of floodplain LW that were/were not in jams and in burned/unburned areas considering only jams that formed within the proximal half of the floodplain width.

The results from these tests show that there is an association between being in a logjam and in the burned area for comparisons 1 and 2, but not for comparison 3 (Table 4). Chi square *p*-values <0.05 indicate that there is an association, and the odds ratio confidence intervals that do not include 1 show that the odds ratio is statistically significant. The odds ratio, λ, is the odds that a piece of LW being in a jam in the burned area is "λ-times" as likely as the odds of a piece of LW being in a jam in the unburned area. For comparison 1 (entire floodplain) and comparison 2 (proximal half of the floodplain), the odds of a piece of LW being in a jam in the burned area is more than two times as likely as in an unburned area. However, comparison 3 (proximal half of the floodplain), fails to reject the null hypothesis that the odds of a piece of LW being in a jam is any different than in the unburned area. These results provide partial, mixed support for H5.

It is difficult to conclude whether H5 appropriately describes the field area. The greater odds of 2.63 for the first 50 m of the floodplain compared to 2.11 for the entire floodplain strengthens the interpretation that the data support H5 because this analysis does not include the jams on the widest part of the floodplain (widest floodplain width is 267 m for subreach 5 transect 4). The results from comparison 3 may or may not be useful because including jams that have traveled ≤50% of the floodplain width (calculated individually for each of the 32 transects) excludes only three pieces of wood from the unburned/in jam group but excludes 19 pieces of wood from the unburned/not in jam group. Because of this and the fact that some of the floodplain transects were very narrow for the floodplain delineated in summer 2019, we put greater interpretive weight on the results from comparisons 1 and 2. Overall, the results support H5.

In summary, the results do not support H1 or H2 because floodplain wood load does not differ significantly between burned and unburned areas of the study reach and floodplain jams are not located closer to the channel. The results support H3 and H4 in that burned wood pieces are present in the channel throughout the study area but are only present in burned portions of the floodplain. The results partly support H5, indicating that a greater proportion of floodplain large wood may be in jams in the burned reaches.

5. Discussion

5.1. Interpretation of hypothesis tests

Overall, the results partly support our hypotheses regarding the movement and storage of LW on floodplain along the Upper Merced River. With respect to differences in wood load between burned and unburned portions of the floodplain (H1), the low number of observations ($n_{transect} = 32$) might have made it difficult to discern a statistical difference. The boxplots in Fig. 4a indicate that with more data points this

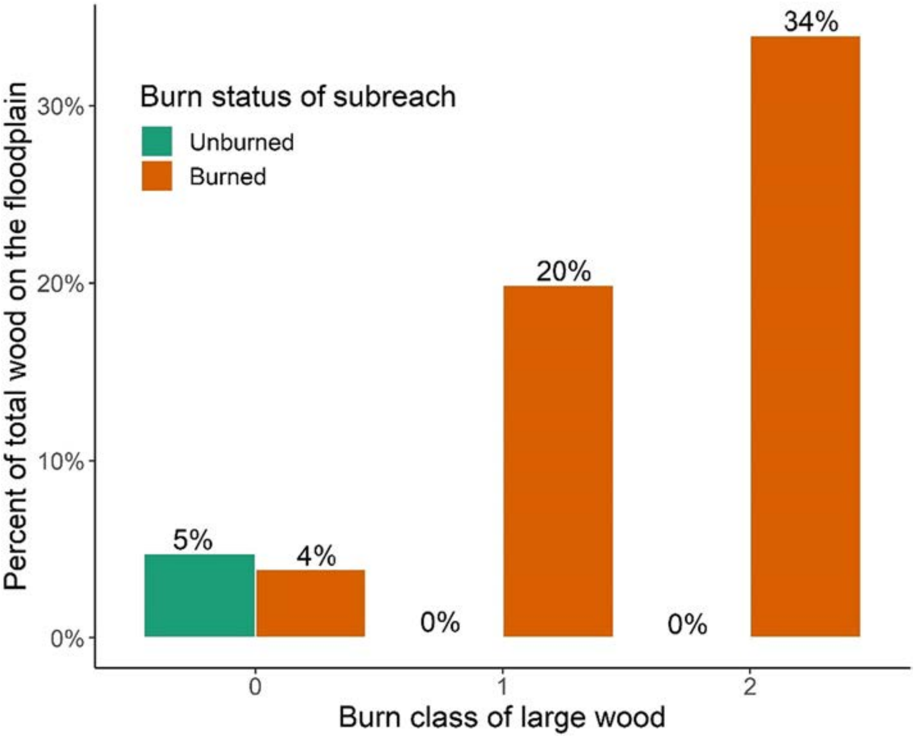

Fig. 7. Burn class of large wood on the floodplain by subreach burn status (H4).

difference in LW loads on the floodplain may prove significant (although it is difficult to tell which area would have the higher wood load). Alternatively, the 2014 fire could have both simultaneously decreased LW load via combustion of downed wood and increased LW load via greater tree mortality and fall, resulting in no statistical difference. More studies on more symmetrical floodplains (in terms of floodplain widths) with differing fire histories would provide insight into the specifics of wood load dynamics.

We respect to the other hypotheses, we infer that different processes drive the dynamics of LW on the floodplain versus in the channel because burned wood was transported through all the subreaches by the flows in the channel (H3) but not on the floodplain (H4) and there is some evidence that LW in burned areas is more likely to become part of a jam than is LW in unburned areas (H5).

We observed patterns in the field that relate these results to the processes of LW dynamics and provide insight into the mechanisms influencing jam distribution that were discussed in the Introduction. First, with respect to bank erosion and logjams, we observed that logjams marginal to the right bank of the Merced River form in predictable places, specifically at the outside of meander bends in sinuous sections of the channel where the channel gradient is lower, such as in subreaches 4 and 5. We also noticed significant bank cutting on the right side of the channel near where these jams accumulate. Key pieces in logjams in the study area are commonly connected to the bank by a root wad. This suggests that the greater flow velocity on the outside of meander bends causes increased tree mortality and topple into the channel via bank erosion, creating wood accumulation in these locations (e.g., Keller and Swanson, 1979; Lassettre et al., 2008). Wood pieces in transport down the channel appear to be trapped by these marginal jams, or sink to the channel bed, based on the observed concentrations of instream wood in marginal jams or as individual pieces on the bed. Where the channel gradient is steeper, such as in subreaches 7 and 8, jams are smaller and there is less bank erosion, suggesting that LW is more effectively transported through these subreaches. Additionally, these steeper subreaches also correspond to greater bedrock exposure along the banks, which limits bank erosion and associated tree topple.

We observed many pieces of LW that were buried along the channel's right bank. We infer that deposition of the LW in jams decreases flow velocities and facilitates sediment deposition on the channel margins and adjacent floodplain, eventually leading to the burial of jams and widening and stabilizing of the riverbank, analogous to the processes described in the floodplain-large wood cycle (Collins et al., 2012). This inference is supported by the tests of H4 and H5 that use burned wood as an indicator for LW transport. Channel jams likely become part of the bank as wood is transported downstream in the channel and laterally onto the floodplain margins, but not longitudinally down the floodplain.

Second, with respect to limited LW transport onto the floodplain because of shallower, slower flows, we found that many of the logjams on the floodplain were concentrated in or near side channels, secondary channels, and abandoned meanders. Similar to the channel, higher flow velocities on the floodplain in these distinct water features likely lead to competent transport of LW across the floodplain, as inferred for floodplain LW depositional sites in other regions (Wohl et al., 2018b). We infer that large wood transport capacity on the floodplain has been more longitudinally and laterally variable than in the channel during the five years since the wildfire because of the intermittency of floodplain inundation and because of the presence of shallow, discontinuous channels in parts of the floodplain. Complex, three-dimensional interactions among floodplain topography, transport capacity, and supply of LW create different wood depositional patterns than those present in the channel. Parts of the floodplain contain numerous jams that are long, narrow, and aligned perpendicular to the river corridor. These jams were commonly held in place by one or more standing trees on the floodplain. We infer that overbank flow creates long, narrow, low jams at locations of reduced wood transport capacity such as the margins of shallow floodplain channels. Wood depositional patterns on the floodplain suggest locally rapid rates of decrease in flow velocity, because of greater relative roughness and shallower flow (Ruiz-Villanueva et al., 2016a), which facilitate formation of long, narrow jams.

5.2. Conceptual model of floodplain wood load after wildfire

Our observations and inferences of floodplain LW dynamics are time-dependent, particularly in the burned zone. Time since wildfire and since last high flow that significantly inundated the floodplain presumably influence what we observed and measured. Fig. 8 conceptually illustrates LW loads in the channel and floodplain with time since disturbance in the form of a wildfire. This model is based on wood loads changing over an interval of 100 years (Wohl, 2011a); a bimodal input of wood to the floodplain forest with an initial input from fire-induced mortality and a second similarly-sized peak after 30 years when the snags fall (Bragg, 2000); a bimodal input of wood to the channel with a small peak right after the fire and a large peak 30 years after (Bragg, 2000); and 255 years for a forest to reach steady state after a major, stand-killing disturbance (Stout et al., 2018). Because of the lack of data for California forests and the fact that wood loads can differ greatly depending on the region, species composition, and characteristics of the river corridor, no values or units are given on the y-axis in Fig. 8. The effects of wildfire on a forest depend on not only the characteristics of the fire, as previously mentioned, but also on the history of drought, beetle kill, and fire suppression and/or maintenance fires, as well as the resistance of trees to fire, rate of tree regrowth, and the pre-fire spatial diversity of the forest (Turner, 2010; Kocher, 2015; National Park Service, 2020).

The Merced River floodplain wood loads are in the upper half of the published values for floodplain wood loads in diverse locations (Fig. 9, Supplemental Table 3). Among these data, only the Yukon River floodplain in Alaska, USA explicitly includes the effect of wildfire. The Alaskan wood loads are much lower than those on the Merced River, but are higher in the burned areas. Greater wood loads on burned floodplains in Alaska likely reflect the fact that boreal fires tend to be of very low intensity, leaving many standing dead trees that gradually topple and creating incomplete combustion of existing downed wood at the time of the fire. Downed wood also has an extremely slow rate of decomposition in the cold, dry conditions of the Yukon River site (Lininger et al., 2017).

The median floodplain wood load of 259 m^3/ha for the Merced River study area is intermediate with respect to floodplain wood loads for other sites in temperate latitudes (the mean value for the Merced River of 250 m^3/ha is reported in Fig. 9 and Supplemental Table 3 in order to be consistent with the other values presented). The wood load is lower than sites with very wet climates and high rates of primary forest productivity (e.g., California redwood, Montana) but higher than wood loads in drier climates in New Mexico and Colorado. This supports previous interpretations that mean annual precipitation and associated forest productivity and wood decay rates may exert a primary control on inter-regional differences in floodplain wood load (Wohl, 2020).

In summary, we cannot conclude from the data and analyses presented here that wildfire significantly influences floodplain wood loads in the study area, although our results suggest that fire can influence the spatial distribution of floodplain LW (Fig. 3) and the concentration of LW pieces in logjams (Table 4).

As progressively more studies document floodplain wood loads and spatial distribution in diverse unmanaged river corridors, the resulting data can be used to inform management designed to restore floodplain large wood in managed river corridors. Activities including timber harvest that reduces the potential for wood recruitment, and flow regulation and channel engineering that geomorphically disconnect channels and floodplains, have resulted in lower wood loads in managed river corridors (Wohl et al., 2017). As river restoration moves beyond

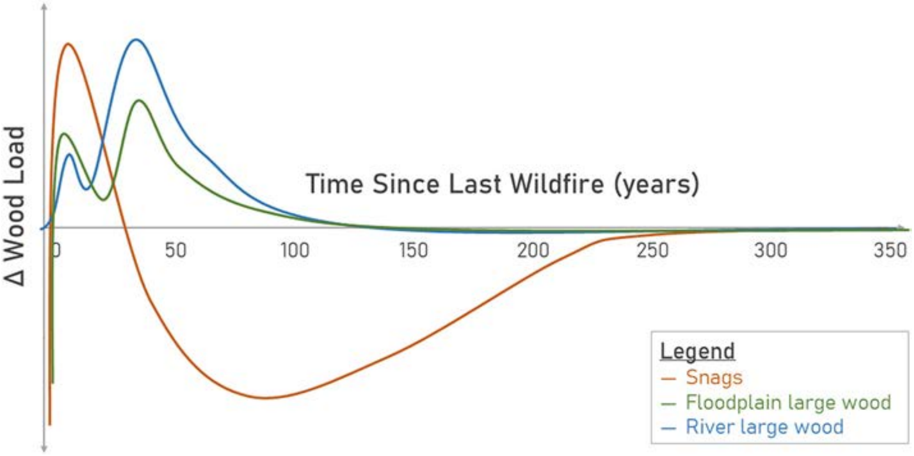

Fig. 8. Conceptual model of changes in wood loads after a stand-killing wildfire.

the active channel to an explicit focus on floodplains (e.g., Tockner et al., 1999; Gourevitch et al., 2020), restoring natural wood regimes or actively emplacing large wood and logjams can create substantial geomorphic and ecological benefits. Knowledge of wood loads and spatial distribution in unmanaged river corridors can be used to define the natural range of variability (Wohl, 2011c) in floodplain wood dynamics.

6. Conclusion

Wildfire may or may not significantly change floodplain wood load, depending on the balance between increased wood recruitment as a result of tree mortality and topple versus consumption of downed wood. In the Merced River, California study area, we found no significant change in wood load between burned and unburned portions of the floodplain. The spatial distribution of wood differs, however, with a greater proportion of pieces within jams in the burned floodplain. The presence of logjams farther from the active channel in the burned floodplain could reflect greater transport capacity because of reduced vegetation density after fire but could also reflect the wider floodplain and presence of secondary channels in the burned floodplain. Floodplain logjams concentrate along the margins of the active channel and in secondary channels in both burned and unburned portions of the floodplain. Given the documented importance of floodplain logjams as habitat for diverse organisms, this suggests the importance of continued

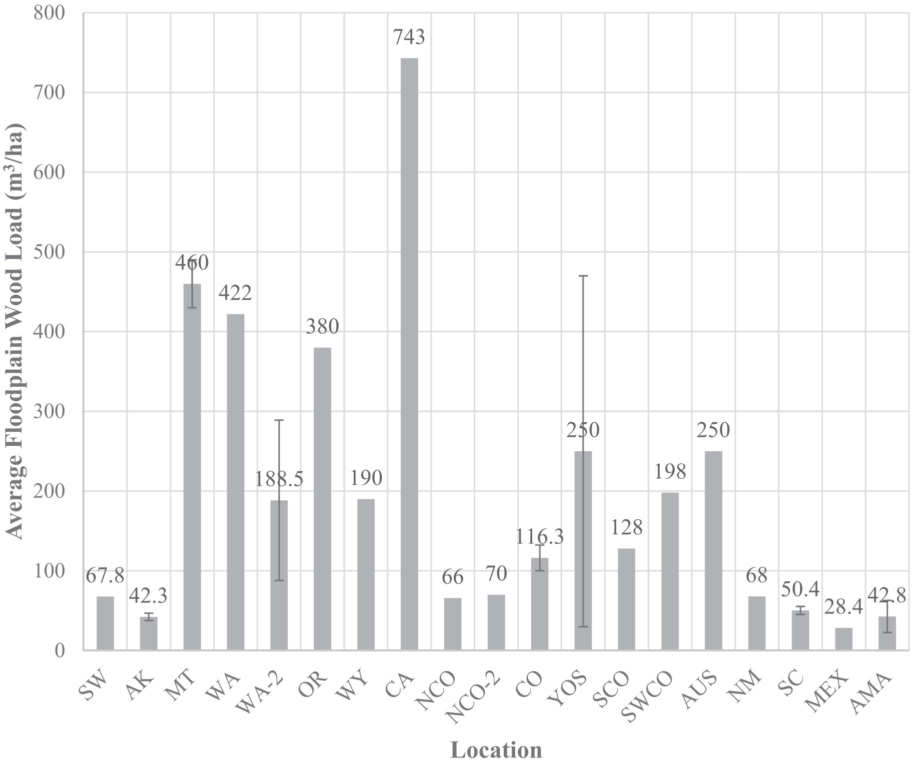

Fig. 9. Average floodplain wood loads for different study areas. Sources and numerical values in Supplemental Table 3. SW = Northern Sweden, AK = Alaska, MT = Montana, WA = Washington (conifer), WA-2 = Washington (rainforest conifer), OR = Oregon, WY = Wyoming, CA = California, NCO = Northern Colorado (montane), NCO-2 = Northern Colorado (subalpine), CO = Colorado, YOS = Merced River study area, SCO = Southern Colorado, SWCO = Southwestern Colorado, AUS = Southeastern Australia, NM = New Mexico, SC = South Carolina, MEX = Central Coast of Mexico, AMA = Western Amazon of Peru. Values shown by the grey bars are the average floodplain wood loads arranged in order of decreasing absolute value of approximate latitude, the vertical bars represent the standard deviation (YOS), the range of the data (MT, WA-2), or the ± given with the published data (AK, CO, SC, AMA). The other locations did not have a range or standard deviation reported.

channel migration in creating floodplain spatial heterogeneity that can facilitate formation of logjams. The median floodplain wood load of 259 m^3/ha for the Merced River study area is intermediate with respect to floodplain wood loads for other sites in temperate latitudes. Continuing studies of floodplain wood load and spatial distribution in unmanaged river corridors can inform management designed to restore geomorphic and ecological effects of large wood in managed river corridors.

Declaration of competing interest

The authors declare that they have no known competing financial interests or personal relationships that could have appeared to influence the work reported in this paper.

Acknowledgements

We would like to acknowledge the funding for this research from the National Park Service, and input received in the form of data, questions, and insight from Mike Martin and Catherine Fong with the National Park Service. We would also like to thank our field assistant Lindsay Floyd, and Ann Hess at Colorado State University for help with the statistics. The manuscript was improved by comments from Francesco Comiti, Herve Piégay, and two anonymous reviewers.

Appendix A. Supplementary data

Supplementary data to this article can be found online at https://doi.org/10.1016/j.geomorph.2021.107805.

References

Aragon, T.J., 2017. epitools: Epidemiology Tools.

Battin, T.J., Kaplan, L.A., Findlay, S., Hopkinson, C.S., Marti, E., Packman, A.I., Newbold, J.D., Sabater, F., 2008. Biophysical controls on organic carbon fluxes in fluvial networks. Nat. Geosci. 1, 95–100. https://doi.org/10.1038/ngeo101.

Beckman, N.D., Wohl, E., 2014. Carbon storage in mountainous headwater streams: the role of old-growth forest and logjams. Water Resour. Res. 50, 2376–2393. https://doi.org/10.1002/2013WR014167.

Benda, L., Miller, D., Bigelow, P., Andras, K., 2003. Effects of post-wildfire erosion on channel environments, Boise River, Idaho. For. Ecol. Manag. 178, 105–119.

Bendix, J., Cowell, C.M., 2010. Fire, floods and woody debris: interactions between biotic and geomorphic processes. Geomorphology 116, 297–304. https://doi.org/10.1016/j.geomorph.2009.09.043.

Benke, A.C., 2001. Importance of flood regime to invertebrate habitat in an unregulated river – floodplain ecosystem. J. N. Am. Benthol. Soc. 20, 225–240.

Berg, N., Azuma, D., Carlson, A., 2002. Effects of wildfire on in-channel woody debris in the Eastern Sierra Nevada, California, in: Proceedings of the Symposium on the Ecology and Management of Dead Wood in Western Forests. USDA Forest Service, Reno, pp. 49–63.

Bocchiola, D., 2011. Hydraulic characteristics and habitat suitability in presence of woody debris: a flume experiment. Adv. Water Resour. 34, 1304–1319. https://doi.org/10.1016/j.advwatres.2011.06.011.

Braccia, A., Batzer, D.P., 2001. Invertebrates associated with woody debris in a Southeastern U.S. forested floodplain wetland. Wetlands 21, 18–31. https://doi.org/10.1672/0277-5212(2001)021[0018:IAWWDI]2.0.CO;2.

Bragg, D.C., 2000. Simulating catastrophic and individualistic large woody debris recruitment for a small riparian system. Ecology 81, 1383–1394. https://doi.org/10.2307/177215.

Brummer, C.J., Abbe, T.B., Sampson, J.R., Montgomery, D.R., 2006. Influence of vertical channel change associated with wood accumulations on delineating channel migration zones, Washington, USA. Geomorphology 80, 295–309.

Chen, X., Wei, X., Scherer, R., 2005. Influence of wildfire and harvest on biomass, carbon pool, and decomposition of large woody debris in forested streams of southern interior British Columbia. For. Ecol. Manag. 208, 101–114.

Collins, B.D., Montgomery, D.R., Fetherston, K.L., Abbe, T.B., 2012. The floodplain large-wood cycle hypothesis: a mechanism for the physical and biotic structuring of temperate forested alluvial valleys in the North Pacific coastal ecoregion. Geomorphology 139–140, 460–470. https://doi.org/10.1016/j.geomorph.2011.11.011.

Comiti, F., Andreoli, A., Mao, L., Lenzi, M.A., 2008. Wood storage in three mountain streams of the Southern Andes and its hydro-morphological effects. Earth Surf. Process. Landf. 33, 244–262.

Dolloff, C.A., Warren Jr., M.L., 2003. Fish relationships with large wood in small streams. In: Gregory, S.V., Boyer, K.L., Gurnell, A.M. (Eds.), The Ecology and Management of Wood in World Rivers, Symposium 37. American Fisheries Society, Bethesda, MD, pp. 179–193.

Donato, D.C., Fontaine, J.B., Campbell, J.L., 2016. Burning the legacy? Influence of wildfire reburn on dead wood dynamics in a temperate conifer forest. Ecosphere 7, e01341.

Dwire, K.A., Kauffman, J.B., 2003. Fire and riparian ecosystems in landscapes of the western USA. For. Ecol. Manag. 178, 61–74. https://doi.org/10.1016/S0378-1127(03)00053-7.

Entrekin, S.A., Rosi, E.J., Tank, J.L., Hoellein, T.J., Lamberti, G.A., 2020. Quantitative food webs indicate modest increases in the transfer of allochthonous and autochthonous C to macroinvertebrates following a large wood addition to a temperate headwater stream. Front. Ecol. Evol. 8, 114.

Fanelli, R.M., Lautz, L.K., 2008. Patterns of water, heat, and solute flux through streambeds around small dams. Ground Water 46, 671–687. https://doi.org/10.1111/j.1745-6584.2008.00461.x.

Fetherston, K.L., Naiman, R.J., Bilby, R.E., 1995. Large woody debris, physical process, and riparian forest development in montane river networks of the Pacific Northwest. Geomorphology 13, 133–144. https://doi.org/10.1016/0169-555X(95)00033-2.

Fox, J., Weisberg, S., 2019. An {R} Companion to Applied Regression. Third. ed. Sage, Thousand Oaks, CA.

Gippel, C.J., 1995. Environmental hydraulics of large woody debris in streams and rivers. J. Environ. Eng. 121, 388–394.

Gourevitch, J.D., Singh, N.K., Minot, J., Raub, K.R., Rizzo, D.M., Wemple, B.C., Ricketts, T.H., 2020. Spatial targeting of floodplain restoration to equitably mitigate flood risk. Glob. Environ. Chang. 61, 102050.

Gurnell, A.M., 2013. Wood in fluvial systems. In: Wohl, E. (Ed.), Fluvial Geomorphology. Academic Press, San Diego, CA, pp. 163–188.

Gurnell, A.M., Piégay, H., Swanson, F.J., Gregory, S.V., 2002. Large wood and fluvial processes. Freshw. Biol. 47, 601–619. https://doi.org/10.1046/j.1365-2427.2002.00916.x.

Gurnell, A.M., Bertoldi, W., Francis, R.A., Gurnell, J., Mardhiah, U., 2019. Understanding processes of island development on an island braided river over timescales from days to decades. Earth Surf. Process. Landf. 44, 624–640.

Hall, A.F. (Ed.), 1921. Handbook of Yosemite National Park: A Compendium of Articles on the Yosemite Region by the Leading Scientific Authorities. G. P. Putnam's Sons, New York.

Herdrich, A.T., Winkelman, D.L., Venarsky, M.P., Walters, D.M., Wohl, E., 2018. The loss of large wood affects Rocky Mountain trout populations. Ecol. Freshw. Fish 27, 1023–1036.

Hess, A., 2019. Statistics 511 and 512 Notes.

Hothorn, T., Hornik, K., van de Wiel, M.A., Zeileis, A., 2006. A Lego system for conditional inference. Am. Stat. 60, 257–263. https://doi.org/10.1198/000313006X118430.

Jeffries, R., Darby, S.E., Sear, D.A., 2003. The influence of vegetation and organic debris on flood-plain sediment dynamics: case study of a low-order stream in the New Forest, England. Geomorphology 51, 61–80. https://doi.org/10.1016/S0169-555X(02)00325-2.

Keller, E.A., Swanson, F.J., 1979. Effects of large organic material on channel form and fluvial process. Earth Surf. Process. 4, 361–380 (doi:0360-1269/79/0404-0361).

Knight, D.W., Shiono, K., 1996. River channel and floodplain hydraulics. In: Anderson, M.G., Walling, D.E., Bates, P.D. (Eds.), Floodplain Processes. Wiley, Chichester, pp. 139–181.

Kocher, S., 2015. California Forests: Presentation to the California Naturalists.

Komsta, L., Novomestky, F., 2015. moments: Moments, Cumulants, Skewness, Kurtosis and Related Tests.

Lassettre, N.S., Piegay, H., Dufour, S., Rollet, A.J., 2008. Decadal changes in the distribution and frequency of wood in a free meandering river, the Ain River, France. Earth Surf. Process. Landf. 33, 1098–1112.

Lautz, L.K., Siegel, D.I., Bauer, R.L., 2006. Impact of debris dams on hyporheic interaction along a semi-arid stream. Hydrol. Process. 20, 183–196. https://doi.org/10.1002/hyp.5910.

Lininger, K.B., Wohl, E., Sutfin, N.A., Rose, J.R., 2017. Floodplain downed wood volumes: a comparison across three biomes. Earth Surf. Process. Landf. 42, 1248–1261. https://doi.org/10.1002/esp.4072.

Livers, B., Wohl, E., 2016. Sources and interpretation of channel complexity in forested subalpine streams of the Southern Rocky Mountains. Water Resour. Res. 52, 3910–3929. https://doi.org/10.1002/2015WR018306.

MacFarlane, W.A., Wohl, E., 2003. Influence of step composition on step geometry and flow resistance in step-pool streams of the Washington Cascades. Water Resour. Res. 39. https://doi.org/10.1029/2001WR001238.

Mao, L., Andreoli, A., Comiti, F., Lenzi, M.A., 2008. Geomorphic effects of large wood jams on a sub-antarctic mountain stream. River Res. Appl. 24, 249–266.

Marcus, W.A., Rasmussen, J., Fonstad, M.A., 2011. Response of the fluvial wood system to fire and floods in northern Yellowstone. Ann. Assoc. Am. Geogr. 101, 21–44.

Nakano, D., Nagayama, S., Kawaguchi, Y., Nakamura, F., 2018. Significance of the stable foundtions provided and created by large wood for benthic fauna in the Shibetsu River, Japan. Ecol. Eng. 120, 249–259.

National Park Service, 2019. Past Fire Activity [WWW Document]. URL https://www.nps.gov/yose/learn/nature/firehistory.htm. (Accessed 14 February 2020).

National Park Service, 2020. Climate Change: Tree Mortality [WWW Document]. URL https://www.nps.gov/yose/learn/nature/cctreemortality.htm (accessed 6.4.20).

Peck, D.L., 1964. Preliminary Geologic Map of the Merced Peak Quadrangle (California).

Peck, D.L., 2002. Geologic Map of the Yosemite Quadrangle, Central Sierra Nevada (California).

Pettit, N.E., Naiman, R.J., 2006. Flood-deposited wood creates regeneration niches for riparian vegetation on a semi-arid South African river. J. Veg. Sci. 17, 615–624. https://doi.org/10.1111/j.1654-1103.2006.tb02485.x.

Picco, L., Scalari, C., Iroume, A., Mazzorana, B., Andreoli, A., 2021. Large wood load fluctuations in an Andean basin. Earth Surf. Process. Landf. https://doi.org/10.1002/esp.5030.

Piégay, H., 1993. Nature, mass and preferential sites of coarse woody debris deposits in the lower Ain Valley (Mollon reach), France. Regul. Rivers Res. Manag. 8, 359–372.

Piégay, H., 2003. Dynamics of wood in large rivers. In: Gregory, S.V., Boyer, K.L., Gurnell, A. M. (Eds.), The Ecology and Management of Wood in World Rivers, Symposium 37. American Fisheries Society, Bethesda, MD, pp. 109–133.

Piégay, H., Gurnell, A.M., 1997. Large woody debris and river geomorphological pattern: examples from S.E. France and S. England. Geomorphology 19, 99–116.

Piégay, H., Marston, R.A., 1998. Distribution of large woody debris along the outer bend of meanders in the Ain River, France. Phys. Geogr. 19, 318–340.

R Core Team, 2019. R: A Language and Environment for Statistical Computing.

Richmond, A.D., Fausch, K.D., 1995. Characteristics and function of large woody debris in subalpine Rocky Mountain streams in northern Colorado. Can. J. Fish. Aquat. Sci. 52, 1789–1802. https://doi.org/10.1139/f95-771.

Ruiz-Villanueva, V., Wyzga, B., Hajdukiewicz, H., Stoffel, M., 2016a. Exploring large wood retention and deposition in contrasting river morphologies linking numerical modelling and field observations. Earth Surf. Process. Landf. 41, 446–459.

Ruiz-Villanueva, V., Piegay, H., Gurnell, A.M., Marston, R.A., Stoffel, M., 2016b. Recent advances quantifying the large wood dynamics in river basins: new methods and remaining challenges. Rev. Geophys. 54, 611–652.

Sawyer, A.H., Cardenas, M.B., Buttles, J., 2012. Hyporheic temperature dynamics and heat exchange near channel-spanning logs. Water Resour. Res. 48, W01529. https://doi.org/10.1029/2011WR011200.

Scott, D.N., Wohl, E.E., 2018. Natural and anthropogenic controls on wood loads in river corridors of the Rocky, Cascade, and Olympic Mountains, USA. Water Resour. Res. 54, 7893–7909.

Sear, D.A., Millington, C.E., Kitts, D.R., Jeffries, R., 2010. Logjam controls on channel:floodplain interactions in wooded catchments and their role in the formation of multichannel patterns. Geomorphology 116, 305–319. https://doi.org/10.1016/j.geomorph.2009.11.022.

Shields, F.D., Smith, R.H., 1992. Effects of large woody debris removal on physical characteristics of a sand-bed channel. Aquat. Conserv. Mar. Freshwat. Ecosyst. 2, 145–163.

Short, L.E., Gabet, E.J., Hoffman, D.F., 2015. The role of large woody debris in modulating the dispersal of a post-fire sediment pulse. Geomorphology 246, 351–358.

Skinner, C.N., Chang, C.-R., 1996. Fire regimes, past and present. Sierra Nevada Ecosystem Project: Final Report to Congress. Davis, pp. 1041–1069.

Stout, J.C., Rutherfurd, I.D., Grove, J., Webb, A.J., Kitchingman, A., Tonkin, Z., Lyon, J., 2018. Passive recovery of wood loads in rivers. Water Resour. Res. 54, 8828–8846. https://doi.org/10.1029/2017WR021071.

Tockner, K., Schiemer, F., Baumgartner, C., Kum, G., Weigand, E., Zweimuller, I., Ward, J.V., 1999. The Danube restoration project: species diversity patterns across connectivity gradients in the floodplain system. Regul. Rivers Res. Manag. 15, 245–258.

Turner, M.G., 2010. Disturbance and landscape dynamics in a changing world. Ecology 91, 2833–2849. https://doi.org/10.1890/10-0097.1.

U.S. Geological Survey, 2020. WaterWatch [WWW Document]. URL. https://waterdata.usgs.gov/ca/nwis.

Van Wagner, C.E., 1968. The line intersect method in forests fuel sampling. For. Sci. 14, 20–26.

Wilcox, A.C., Wohl, E.E., Comiti, F., Mao, L., 2011. Hydraulics, morphology, and energy dissipation in an alpine step-pool channel. Water Resour. Res. 47, W07514. https://doi.org/10.1029/2010WR010192.

Wohl, E., 2011a. Seeing the forest and the trees: wood in stream restoration in the Colorado Front Range, United States. Geophys. Monogr. Ser. 194, 399–418. https://doi.org/10.1029/2010GM000987.

Wohl, E., 2011b. Threshold-induced complex behavior of wood in mountain streams. Geology 39, 587–590.

Wohl, E., 2011c. What should these rivers look like? Historical range of variability and human impacts in the Colorado Front Range, USA. Earth Surf. Process. Landf. 36, 1378–1390.

Wohl, E., 2013. Floodplains and wood. Earth Sci. Rev. 123, 194–212. https://doi.org/10.1016/j.earscirev.2013.04.009.

Wohl, E., 2016. Spatial heterogeneity as a component of river geomorphic complexity. Prog. Phys. Geogr. 40, 598–615. https://doi.org/10.1177/0309133316658615.

Wohl, E., 2017. Bridging the gaps: an overview of wood across time and space in diverse rivers. Geomorphology 279, 3–26. https://doi.org/10.1016/j.geomorph.2016.04.014.

Wohl, E., 2020. Wood process domains and wood loads on floodplains. Earth Surf. Process. Landf. 45, 144–156. https://doi.org/10.1002/esp.4771.

Wohl, E., Cenderelli, D.A., Dwire, K.A., Ryan-Burkett, S.E., Young, M.K., Fausch, K.D., 2010. Large in-stream wood studies: a call for common metrics. Earth Surf. Process. Landf. 35, 618–625. https://doi.org/10.1002/esp.1966.

Wohl, E., Lininger, K.B., Fox, M., Baillie, B.R., Erskine, W.D., 2017. Instream large wood loads across bioclimatic regions. For. Ecol. Manag. 404, 370–380.

Wohl, E., Scott, D.N., Lininger, K.B., 2018. Spatial distribution of channel and floodplain large wood in forested river corridors of the Northern Rockies. Water Resour. Res. 54, 7879–7892.

Wohl, E., Cadol, D., Pfeiffer, A., Jackson, K., Laurel, D., 2018a. Distribution of large wood within river corridors in relation to flow regime in the semiarid western US. Water Resour. Res. 54, 1890–1904.

Wohl, E., Kramer, N., Ruiz-Villanueva, V., Scott, D.N., Comiti, F., Gurnell, A.M., Piegay, H., Lininger, K.B., Jaeger, K.L., Walters, D.M., Fausch, K.D., 2019. The natural wood regime in rivers. BioScience 69, 259–273.

Wohl, E., Lininger, K.B., Rathburn, S.L., Sutfin, N.A., 2020. How geomorphic context governs the influence of wildfire on floodplain organic carbon in fire-prone environments of the western United States. Earth Surf. Process. Landf. 45, 38–55.

Young, M.K., 1994. Movement and characteristics of stream-borne coarse woody debris in adjacent burned and unburned watersheds in Wyoming. Can. J. For. Res. 24, 1933–1938.

Zalewski, M., Lapinska, M., Bayley, P.B., 2003. Fish relationships with wood in large rivers. In: Gregory, S.V., Boyer, K.L., Gurnell, A.M. (Eds.), The Ecology and Management of Wood in World Rivers, Symposium 37. American Fisheries Society, Bethesda, MD, pp. 195–211.

Zelt, R.B., Wohl, E.E., 2004. Channel and woody debris characteristics in adjacent burned and unburned watersheds a decade after wildfire, Park County, Wyoming. Geomorphology 57, 217–233.